Characterization of local deformation and fracture behavior in ferrite + martensite dual-phase steels having different grain sizes

M H Park[1], Y Tagusari[1] and N Tsuji[1, 2]

[1] Department of Materials Science and Engineering, Kyoto University, Yoshida Honmachi, Sakyo-ku, Kyoto 606-8501, Japan
[2] Elements Strategy Initiative for Structural Materials (ESISM), Kyoto University, Yoshida Honmachi, Sakyo-ku, Kyoto 606-8501, Japan

E-mail: park.myeongheom.8r@kyoto-u.ac.jp

Abstract. Low carbon dual-phase (DP) steels composed of soft ferrite and hard martensite have been widely used in the automotive industry due to their good strength-ductility balance and large strain hardening ability. DP steels have a wide variation in mechanical properties depending on several microstructural features such as grain size, phase fraction and distribution. Among them, the grain refinement of DP steels is known to be an effective option for enhancing mechanical performance in strength and ductility (especially post-uniform elongation). However, the exact reason for the significant improvement of post-uniform elongation by grain refinement has not been fully understood. It is considered that the characterization of local deformation behavior and micro-void formation/growth behavior in connection with microstructures is an essential approach for understanding the enhanced post-uniform elongation realized in the fine-grained DP specimen. In the present study, we prepared two kinds of DP specimens with mean ferrite grain sizes of 14.9 μm (coarse-grained DP) and 7.1 μm (fine-grained DP), and carefully investigated local strain distribution of tensile specimen and micro-void formation/growth behavior using digital image correlation (DIC) analysis and SEM observations. The fine-grained DP specimen exhibited a gradual strain localization after necking and had sufficient strain capacity that could endure against fracture. The fine-grained DP structure had a great number of micro-voids in the necked region, but almost all the micro-voids maintained a very small size, which was contrasted with the case of coarse-grained DP specimen containing very large-sized micro-voids. Such a significant difference in micro-void size/number characters between two kinds of DP specimens would be one possible reason for exhibiting greatly different post-uniform elongation behavior.

1. Introduction

Steels used for structural materials have been increasingly required to manage both high strength and large ductility for the safety of structural applications and the achievement of high fuel-efficiency through the reduction of body weight of automobile components. Dual-phase (DP) steels consisting of soft ferrite phase and hard martensite phase are widely used steels due to their good mechanical balance between strength and ductility. Over several decades, many studies of DP steels have been achieving much better mechanical performance by changing microstructural factors such as phase distribution, grain size, phase strength (hardness) and phase fraction [1-3]. Recently, it has been found that the grain refinement for DP steels is a promising strategy to simultaneously improve strength and ductility

(especially post-uniform elongation) [2, 4]. However, the underlying reason for the enhancement of post-uniform elongation realized by grain refinement is still not fully understood. The characterization of local deformation behavior including micro-void evolution can be one effective approach for understanding the overall deformation-fracture nature of DP structures [5, 6]. In the present study, we characterize the local deformation behavior of DP tensile specimens by means of the digital image correlation (DIC) technique providing strain distribution maps, and then investigate the micro-void size and its number by SEM observation for tensile-fractured DP specimens having different grain sizes.

2. Experimental procedures

A low carbon steel having a chemical composition of Fe-2Mn-0.1C (mass%) was used in the current study. Ae3 and Ae1 temperatures of the present alloy were calculated to be 804 ℃ and 655 ℃, respectively, using Thermo-Calc software with TCFE7.0 thermodynamic database. Specimens were austenitized at two different temperatures of 950 ℃ and 810 ℃ for 3 hr, followed by furnace cooled (F.C.) in a vacuum condition for obtaining ferrite + pearlite microstructures having different ferrite grain sizes. Afterward, ferrite + martensite DP structure was obtained from ferrite + austenite intercritical annealing at 750 ℃ for 2 hr, followed by water quenching (W.Q.), during which austenite was transformed to martensite. Microstructure observation was carried out using a field-emission scanning electron microscope (FE-SEM, JEOL JSM 7100F) equipped with an electron back-scattered diffraction (EBSD) system at an accelerated voltage of 15kV. The specimen for SEM observation was prepared through mechanical polishing with 400-4000 grid-sized emery papers and subsequent electrolytic polishing in a chemical solution of 90 vol% of CH_3COOH and 10 vol. % of $HClO_4$ with a voltage of 22 V for 30 s at room temperature. Tensile properties were evaluated using a uniaxial tensile testing machine (Shimadzu, AG-100kN Xplus) with an initial strain rate of 8.3×10^{-4} s^{-1} at room temperature. Tensile specimen with a gauge length of 10 mm, gauge width of 5 mm and thickness of 1 mm was cut from the heat-treated sheets. Tensile displacement (or strain) of gauge and strain distribution of tensile specimen were accurately measured by the digital image correlation (DIC) technique. For DIC strain analysis, a speckle pattern was introduced on the surface of the tensile specimen with white and black inks prior to the tensile test. The images including tensile specimen were captured by a CCD camera (SVS-VISTEK) with a constant speed of 5 fps during the tensile test, and they were provided for DIC analysis software (Correlated solutions Inc., Vic-2D) to obtain a strain distribution map. The size and number of micro-voids were investigated by careful SEM observation with the tensile-fractured DP specimens, for which a dedicated image-processing software (ImageJ) was utilized.

3. Results and discussion

3.1. Microstructural characteristic and tensile properties

Figure 1 exhibits SEM-EBSD image quality (IQ) maps and corresponding kernel average misorientation (KAM) maps of the DP specimens obtained from the heat treatments of (a) 950 ℃-3hr-F.C. + 750 ℃-2hr-W.Q. and (b) 810 ℃-3hr-F.C. + 750 ℃-2hr-W.Q. Contrast on IQ map reflects diffraction pattern quality of Kikuchi line, and colors on KAM map indicate KAM value according to the key KAM color bar. Since the martensite containing a high density of lattice defects lead to lower IQ value (darker contrast in IQ map) and higher KAM value, ferrite and martensite can be distinguished with such differences in IQ map and KAM map. Capital letters **F** and **M** on the IQ map are ferrite and martensite, respectively. The specimen (a) and specimen (b) in figure 1 exhibited different mean ferrite grain size of 14.9 μm and 7.1 μm, respectively, but they had almost the same martensite fraction (f_M = 45% for the specimen (a) and f_M = 46% for the specimen (b)) and similar martensite distribution with chain-shaped martensite surrounding ferrite grains, each of which will be referred to as “coarse-grained DP” and “fine-grained DP” hereafter.

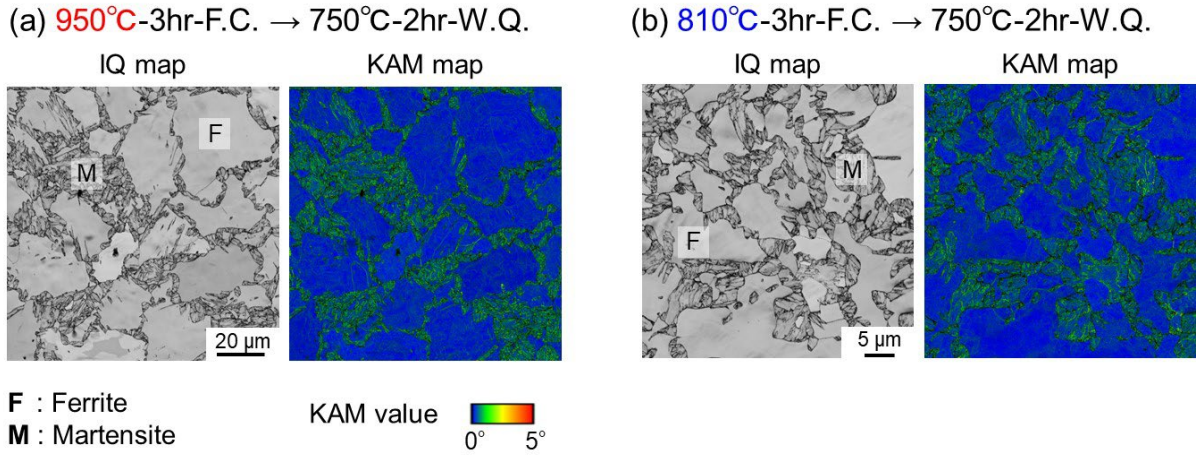

Figure 1. EBSD image quality (IQ) maps and corresponding kernel average misorientation (KAM) maps of DP specimens obtained from the heat treatments of (a) 950 ℃-3hr-F.C. + 750 ℃-2hr-W.Q. and (b) 810 ℃-3hr-F.C. + 750 ℃-2hr-W.Q. **F** and **M** on IQ map denote ferrite and martensite, respectively, and colors on KAM map indicate KAM value according to the key color bar.

Figure 2 displays nominal stress-strain (S-S) curves of the coarse-grained DP specimen (red) and the fine-grained DP specimen (blue). The circle symbol on each S-S curve indicates S-S point at uniform elongation. The fine-grained DP specimen exhibited a higher yield strength (0.2% proof stress) of 410 MPa and ultimate tensile strength (UTS) of 801 MPa than the coarse-grained DP specimen having a yield strength of 374 MPa and a UTS of 734 MPa. The fine-grained DP specimen exhibited much better ductility with a uniform elongation of 0.107 and a post-uniform elongation of 0.104 than the coarse-grained DP specimen (uniform elongation of 0.106 and post-uniform elongation of 0.072), indicating that grain refinement of DP structure greatly enhanced post-uniform elongation as well as high strength. We further investigated the local deformation behavior of tensile specimens in the period of post-uniform elongation using DIC strain analysis.

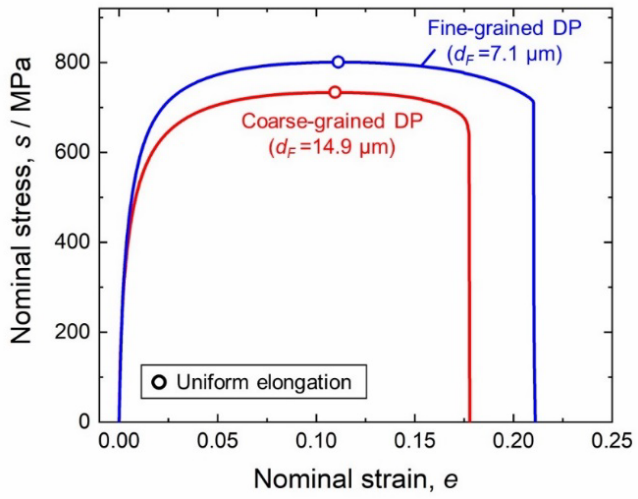

Figure 2. Nominal stress-strain curves of coarse-grained DP specimen (red) and fine-grained DP specimen (blue). Circle symbol on the curve corresponds to uniform elongation of each DP specimen.

Figure 3 shows the DIC strain distribution maps of (a) coarse-grained DP and (b) fine-grained DP tensile specimens at specific global tensile strains (nominal strain). The tensile direction is parallel to the vertical direction of images, and the colors superimposed on the tensile specimens correspond to the value of normal strain in the tensile direction (ε_{yy}), according to the key strain color bar. It was found that two kinds of tensile specimens showed rather homogeneous strain distributions in the gauge part until the global tensile strain of 10%. At a global tensile strain of 15%, a clear strain-localized band was observed in both DP tensile specimens, and a sharp difference in the magnitude of strain localization was recognized at the further tensile-strained condition of 17.8%. The maximum local strain value in the necked region of the coarse-grained DP specimen was 0.65 at the global tensile strain of 17.8%, whereas that of the fine-grained one was 0.44 at the same global tensile strain. The fine-grained DP specimen could be further tensile-deformed to the global tensile strain of 21.1%, in which the maximum local strain in the necked region was reached to 0.90.

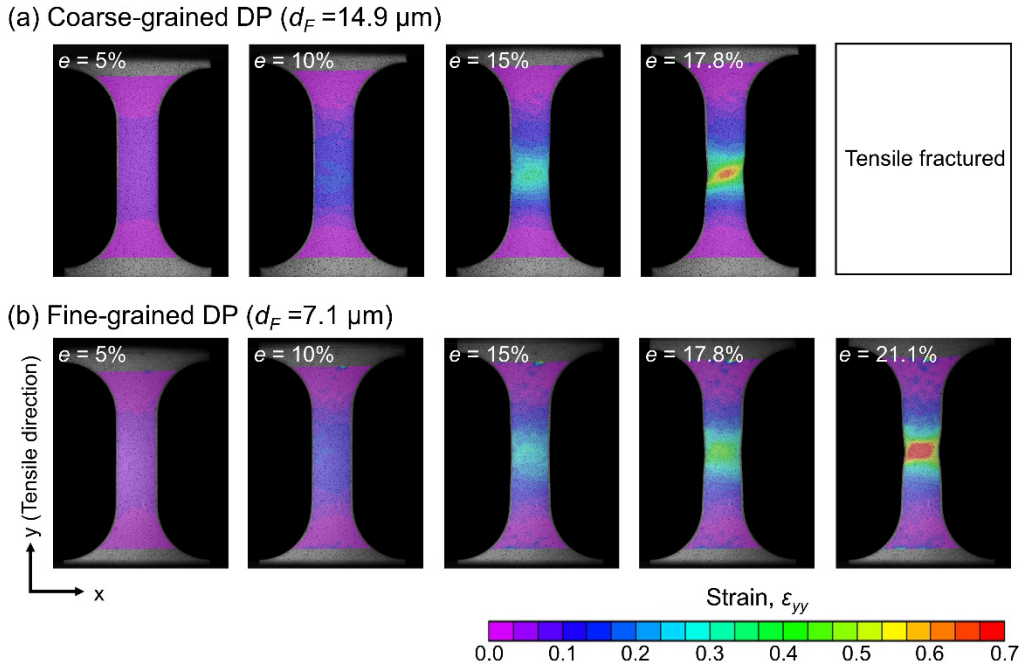

Figure 3. DIC strain distribution maps of (a) coarse-grained DP and (b) fine-grained DP tensile specimens at the nominal strain of 5%, 10%, 15%, 17.8% and 21.1%. Colors superimposed on the tensile specimen correspond to the normal strain value in tensile direction (ε_{yy}), according to key strain color bar.

Figure 4 displays local strain (ε_{yy}) changes at the strain-inspection point as a function of global tensile strain (i.e., nominal strain). The local strain data were extracted from the DIC strain distribution results in figure 3, and the strain-inspection point was set on the most strain-localized region. An X-mark on the graph indicates tensile-failure, and a broken line is a one-to-one correspondence line of global tensile strain and local strain (i.e., homogeneous deformation line). In both DP specimens, the local strain linearly increased along the homogeneous deformation line until around 10% global tensile strain. After that, in both specimens, the local strain showed an exponential increase, greatly deviating from the homogeneous deformation line. The fine-grained DP specimen exhibited a more gradual increase of local strain, and eventually had a much larger strain capacity that could endure against tensile failure. It is believed that such a significantly different strain localization manner between coarse-grained DP and fine-grained DP specimens can be understood by investigating microstructural deformation behavior including micro-void evolution in the strain-localized region.

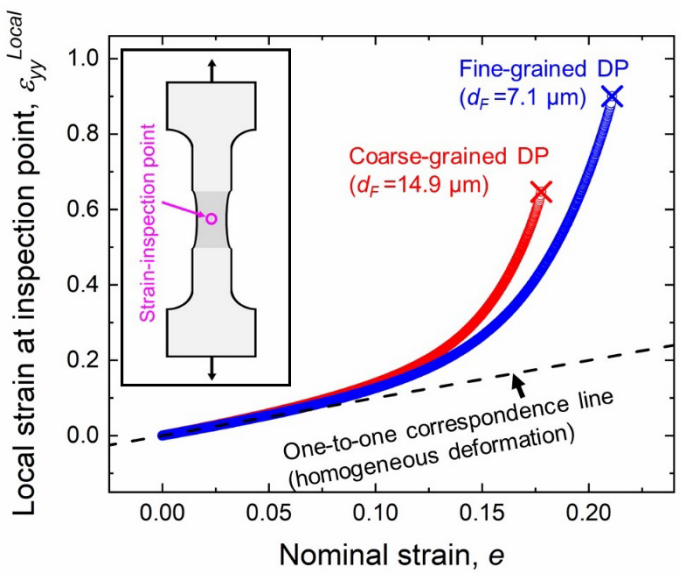

Figure 4. Local strain change at the strain-inspection point in coarse-grained DP (red) and fine-grained DP (blue) tensile specimens as a function of nominal strain. The Strain-inspection point was set on the most strain-localized region.

3.2. Micro-void characterization in the strain-localized region

Figure 5 shows micro-void characterization results investigating (a) the size of each micro-void and (b) the number of micro-voids in the observed area at a tensile-directional distance from the fracture surface of tensile-fractured DP specimens. The schematic illustration of the observed position is inserted in both graphs. Note that, in figure 5 (a), each data point indicates the size for an individual micro-void, and the size is evaluated as an area unit (μm^2) of each micro-void. It was found that in figure 5 (a) that almost all the micro-voids observed in both DP specimens had a quite small void size less than 10 μm^2 even in the vicinity of the fracture surface. It was noteworthy that large-sized micro-voids ranging from 20 μm^2 to 70 μm^2 were observed only in the coarse-grained DP specimen, which intensively occurred near fracture surface. This suggests that several large-sized micro-voids formed in the coarse-grained DP specimen give more critical chances to lead to relatively early tensile failure. In the result of Figure 5 (b) investigating the number of micro-voids, it was found in both DP specimens that a great number of micro-voids were observed in the vicinity of the fracture surface, and the number of them were significantly decreased as a distance from the fracture surface. On the other hand, the absolute number of micro-voids in the vicinity of the fracture surface was apparently different between coarse-grained DP and fine-grained DP specimens. It is intriguing that the fine-grained DP specimen exhibiting larger post-uniform elongation has five times more micro-voids (n_{void} = 62) than the coarse-grained DP specimen (n_{void} = 12) at the position of 150 μm from the fracture surface. A great number of micro-voids in the fine-grained DP specimens just before fracture might be related to its very large local strain value in the necked region of the tensile specimen. Considering that the fine-grained DP specimen exhibits a gradual strain increase even after necking as shown in figure 3, profusely distributed micro-void formation sites such as grain boundaries and interface may lead to delocalizing microscopic strains. We believe that the reason for such a large number of micro-void formations in the fine-grained DP specimen can be understood by characterizing microscopic deformation behavior through the microscopic DIC (μ-DIC) technique. The finding(s) combined with μ-DIC microstructure strain result will show a great synergy for the global view of the deformation nature of DP structure in connection

with global mechanical response, leading to effective material design strategy that can realize a simultaneous improvement of strength and ductility in DP structures.

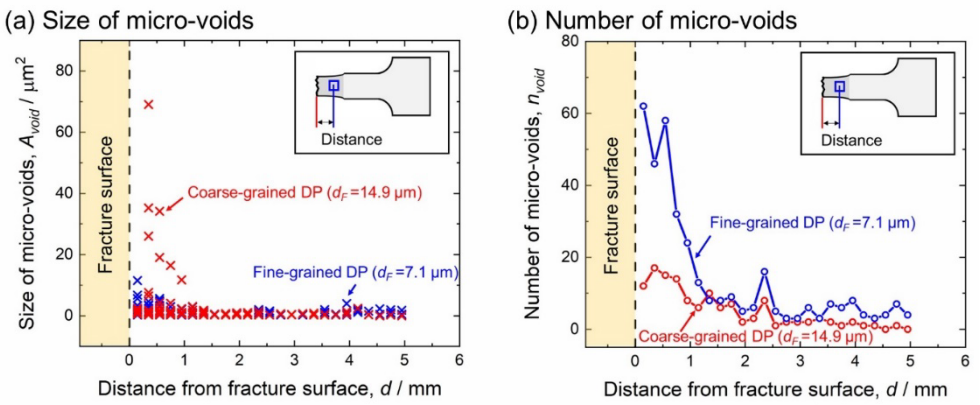

Figure 5. Characterization of micro-voids in tensile-fractured DP specimens having a mean ferrite grain size of 14.9 μm (red) and 7.1 μm (blue): (a) Size and (b) number of micro-voids as a function of distance from the fracture surface.

4. Conclusions

In the present study, local deformation behavior and micro-void characterization of DP specimens having different ferrite grain sizes were investigated using DIC analysis and SEM observation. DP specimen having a mean ferrite grain size of 7.1 μm (fine-grained DP) exhibited an excellent mechanical balance between strength and ductility (especially post-uniform elongation), compared to the coarse-grained DP specimen having a mean ferrite grain size of 14.9 μm. From the result of the DIC strain distribution of tensile specimen, the fine-grained DP specimen showed a slow strain localization and large strain localization capacity against fracture, which might be one of the possible reasons for the enhancement of post-uniform elongation of fine-grained DP specimen. In microstructure observation, a great number of small-sized micro-voids were observed in the fine-grained DP specimen, which indicated that micro-void growth can be effectively inhibited by grain refinement in DP structure.

References

[1] Delincé M, Bréchet Y, Embury J D, Geers M G D, Jacques P J and Pardoen T 2007 Structure-property optimization of ultrafine-grained dual-phase steels using a microstructure-based strain hardening model, *Acta Mater.* **55** 2337–50
[2] Park M H, Shibata A and Tsuji N 2016 Effect of Grain Size on Mechanical Properties of Dual Phase Steels Composed of Ferrite and Martensite, *MRS Adv.* **1** 811–6
[3] Mazinani M and Poole W J 2007 Effect of martensite plasticity on the deformation behavior of a low-carbon dual-phase steel, *Metall. Mater. Trans. A* **38** 328–39
[4] Calcagnotto M, Adachi Y, Ponge D and Raabe D 2011 Deformation and fracture mechanisms in fine- and ultrafine-grained ferrite/martensite dual-phase steels and the effect of aging, *Acta Mater.* **59** 658–70
[5] Azuma M, Goutianos S, Hansen N, Winther G and Huang X 2012 Effect of hardness of martensite and ferrite on void formation in dual phase steel, *Mater. Sci. Technol.* **28** 1092–1100
[6] Saeidi N, Ashrafizadeh F, Niroumand B, Forouzan M R, Mohseni M S and Barlat F 2015 Void coalescence and fracture behavior of notched and un-notched tensile tested specimens in fine grain dual phase steel, *Mater. Sci. Eng.* A **644** 210-7